

## Catalytic abatement of CO and VOCs in waste gases over alumina-supported Cu-Mn catalysts modified by cobalt

E. N. Kolentsova<sup>1</sup>, D. Y. Dimitrov<sup>1</sup>, D. B. Karashanova<sup>2</sup>, Y. G. Karakirova<sup>3</sup>, P. Ts. Petrova<sup>3</sup>,  
T. T. Tabakova<sup>3,\*</sup>, G. V. Avdeev<sup>4</sup>, K. I. Ivanov<sup>1</sup>

<sup>1</sup> Department of Chemistry, Agricultural University, 4000 Plovdiv, Bulgaria

<sup>2</sup> Institute of Optical Materials and Technologies, Bulgarian Academy of Sciences, 1113 Sofia, Bulgaria

<sup>3</sup> Institute of Catalysis, Bulgarian Academy of Sciences, 1113 Sofia, Bulgaria

<sup>4</sup> Institute of Physical Chemistry, Bulgarian Academy of Sciences, 1113 Sofia, Bulgaria

Received: February 01, 2018; Revised: March 11, 2018

Production of formaldehyde by selective oxidation of methanol is an important industrial process. The main by-products in the waste gases are CO and dimethyl ether (DME). Currently, rational design of new catalytic materials with improved efficiency in the removal of air pollutants is a topic of appreciable research. The aim of this study was to combine advantages of both Cu-Mn and Cu-Co catalytic systems by obtaining a new mixed Cu-Mn-Co catalyst of high activity and selectivity in the simultaneous oxidation of CO, methanol, and DME. XRD, TEM, EPR and TPR techniques were used to characterise prepared samples.

**Key words:** Copper-manganese-cobalt catalyst, CO and VOCs oxidation.

### INTRODUCTION

Catalytic oxidation is a widely applied and effective method of removing toxic components such as CO and volatile organic compounds (VOCs) emitted by transport activities, and petrochemical and chemical industries [1–4], including formalin production by selective oxidation of methanol [5]. Many studies have shown that precious metals such as Pt, Pd, Au, and Ag [2,3] demonstrate high activity at a relatively low temperature, but are more expensive and some of the problems associated with their industrial exploitation (such as low stability, particle agglomeration, and susceptibility to poisoning) limit their wide application. On the other hand, transition metal oxides (Fe<sub>2</sub>O<sub>3</sub>, Co<sub>3</sub>O<sub>4</sub>, NiO, Cr<sub>2</sub>O<sub>3</sub>, CuO, and MnO<sub>2</sub>) are subject to significant studies [2,4,6]. Advantages of these catalysts are related to lower costs, but also to higher thermal stability and resistance to catalytic poisons, which is essential for their performance [4,7]. At low temperatures, they are less active than precious metal catalysts; however, some specific combinations of metal oxides may improve their activity in VOC elimination reactions [2]. For example, Faure *et al.* [8] have investigated Cu-Co catalysts for catalytic oxidation of model VOCs (toluene and ethyl acetate) prepared by the precipitation method. The results indicated the presence of synergistic

effect between copper and cobalt in the mixed Cu-Co oxide catalysts, which showed a higher activity compared to copper oxide or cobalt oxide. According to the authors, finely divided copper particles on a Co<sub>3</sub>O<sub>4</sub> surface especially in the Cu-Co spinel is the most likely reason of increased specific surface area and improved catalytic activity regarding VOC oxidation. According to other authors, mixed spinel-type Co-Mn oxides that have better oxidation properties than Co<sub>3</sub>O<sub>4</sub> concerned with VOC complete oxidation [9] are produced by partial replacement of cobalt by manganese. Cu-Mn catalysts have also been shown to be effective in the oxidation reaction of CO [10–12], a wide range of VOCs [13–15], water-gas shift reaction [16], methanol steam reforming [17], etc. Own studies [15] have revealed that alumina-supported mixed Cu-Mn oxide catalysts manifest an increased activity with respect to the oxidation of CO, methanol and DME. A synergistic interaction between copper and manganese species was observed to increase the activity for total oxidation of tested toxic components compared to the activity of CuO/ $\gamma$ -Al<sub>2</sub>O<sub>3</sub> and MnO<sub>x</sub>/ $\gamma$ -Al<sub>2</sub>O<sub>3</sub> catalysts. It has been found that carrier type, calcination temperature, and active phase composition are important factors influencing the catalytic activity [15]. Due to mentioned properties nanosized mixed spinel-type oxides have been extensively studied in recent decades [1,13]. Improved properties of mixed oxides against individual oxides are well known especially in environmental catalysis [1,15]. Spinel

\* To whom all correspondence should be sent  
E-mail: tabakova@ic.bas.bg

materials, however, are quite sensitive to synthesis conditions, which may affect both morphological and structural properties [1,10]. Therefore, one of the major challenges associated with this type of material is to find appropriate preparation methods leading to defects in nanocrystalline particles, which may favour catalytic performance [1].

The main idea of this study is to combine advantages of the Cu-Mn and Cu-Co catalytic systems by producing new mixed Cu-Mn-Co oxide catalysts with spinel structure that exhibit high activity and selectivity for simultaneous oxidation of CO, methanol, and DME, which are waste products in formaldehyde production.

## EXPERIMENTAL

### *Catalyst preparation*

A copper-rich Cu-Mn/ $\gamma$ -Al<sub>2</sub>O<sub>3</sub> sample of Cu/Mn molar ratio of 2:1 and a manganese-rich sample of Cu-Mn molar ratio of 1:5 were selected for this investigation. Manganese in these samples was replaced by cobalt in the entire concentration range. Catalyst preparation was carried out by impregnation of  $\gamma$ -alumina support (80 wt.%, fraction 0.6–1.0) with aqueous solution of copper, cobalt, and manganese nitrates of different composition. The total amount of active phase was 20 wt.%. Before impregnation, the carrier was calcined for 2 hours at 450 °C in a ceramic furnace. After keeping at room temperature, earlier prepared solutions of copper, manganese, and cobalt nitrates were added. The support remained immersed in the salt solution for 12 hours at 80 °C. After the impregnation, the samples were dried and calcined in the following sequence: drying for 12 h at room temperature, heating at 120 °C for 10 h, and raising the temperature at 10 °C/min to 450 °C where it was held for 4 hours.

### *Analytical techniques for sample characterisation*

X-ray powder diffraction (XRD) patterns for phase identification were recorded on a Philips PW 1050 diffractometer equipped with Cu K $\alpha$  tube and scintillation detector. Data on cell refinements were collected in  $\theta$ -2 $\theta$  step-scan mode in the angle interval from 10 to 90° (2 $\theta$ ) at steps of 0.03° (2 $\theta$ ) and counting time of 3 s/step. The cell refinements were obtained with PowderCell program. Size-strain analysis was carried out using BRASS-Bremen Rietveld Analysis and Structure Suite.

Transmission electron microscopy (TEM) measurements were performed by a JEOL JEM 2100 instrument at accelerating voltage 200 kV. Selected Area Electron Diffraction (SAED) was also

employed to gain information on the nature of the crystalline phases.

Temperature-programmed reduction (TPR) of the samples was carried out in a flow system under the following conditions: hydrogen-argon gas mixture (10 vol.% H<sub>2</sub>), temperature ramp of 15 °C/min, flow rate of 24 ml/min, and sample amount of 0.05 g.

EPR spectra were recorded on a JEOL JES-FA 100 EPR spectrometer operating in X-band with standard TE<sub>011</sub> cylindrical resonator under the following conditions: modulation frequency of 100 kHz, microwave power of 1 mW, modulation amplitude of 0.2 mT, sweep of 500 mT, time constant of 0.3 s, and sweeping time of 4 min.

The catalytic measurements of single compounds oxidation were performed by continuous flow equipment with a four-channel isothermal stainless steel reactor containing 1.0 ml catalyst at atmospheric pressure and space velocity (GHSV) of 10000 h<sup>-1</sup> allowing simultaneous examination of four samples under the same conditions. A flow of ambient air (40–50% humidity) and CO (final concentration of 2.0%), and mass flow controllers (GFC Mass Controller AABORG, Germany) were used. Liquid methanol was cooled to 0 °C in evaporator through which a stream of air was passed. Additional air was added after the evaporator to final concentration of methanol 2.0 vol.%. DME (final concentration 0.8–1.0 vol.%) was obtained by dehydration of methanol in nitrogen flow on  $\gamma$ -Al<sub>2</sub>O<sub>3</sub> in tubular isothermal reactor. Gas mixtures at reactor inlet and outlet were analysed by means of a HP 5890 Series II gas chromatograph equipped with FID and TCD detectors, Porapak Q column (for methanol, CO<sub>2</sub>, and DME), and MS-5A column (for CO, oxygen, and nitrogen).

## RESULTS AND DISCUSSION

### *Powder X-ray diffraction*

Samples of the Cu-Mn/ $\gamma$ -Al<sub>2</sub>O<sub>3</sub> series of Cu/Mn ratio in the active phase of 2:1 or 1:5, in which manganese was partly or completely replaced by cobalt, were analysed by XRD. The samples were selected after evaluation of the catalytic behaviour in CO, methanol, and DME oxidation.

X-ray diffraction patterns of the Cu-Mn/ $\gamma$ -Al<sub>2</sub>O<sub>3</sub> series samples with Cu/Mn in the active phase of 1:5 (a), in which manganese was replaced by cobalt (40, 60, and 100%), are shown in Fig. 1 (A). For comparison, XRD patterns of samples containing alumina-supported MnO<sub>2</sub> (e) or Co<sub>3</sub>O<sub>4</sub> (f) as well as of the  $\gamma$ -Al<sub>2</sub>O<sub>3</sub> support (h) are presented. The intensity of the peaks due to formation of separate phase

of  $\text{Co}_3\text{O}_4$  (Ref. Code 98-015-0805) at  $2\theta = 31.2, 36.9, 44.7, 55.8, 59.5,$  and  $65.5^\circ$  increased upon increasing its amount, however, comparison with  $\text{Co}_3\text{O}_4/\gamma\text{-Al}_2\text{O}_3$  sample (f) revealed a higher dispersion of the  $\text{Co}_3\text{O}_4$  phase in the  $\text{Cu-Mn-Co}/\gamma\text{-Al}_2\text{O}_3$  samples. Replacement of Mn by Co caused a significant decrease of the reflections of  $\text{MnO}_2$  at  $2\theta = 28.6, 37.2, 42.8,$  and  $56.5^\circ$ .

XRD patterns of the  $\text{Cu-Mn}/\gamma\text{-Al}_2\text{O}_3$  samples (Cu/Mn ratio of 2:1 or 1:5) in which manganese was completely replaced by cobalt are compared in Fig. 1 (B). The dominating reflections for the  $\text{Co}_3\text{O}_4$  phase are well visible in the pattern of the sample of 1:5 ratio. The most intense reflections at  $2\theta = 35.6$  and  $38.8^\circ$ , typical of  $\text{CuO}$ , were registered in the patterns of the Cu-Co sample of 2:1 ratio.

### Transmission electron microscopy

Results of transmission electron microscopy of

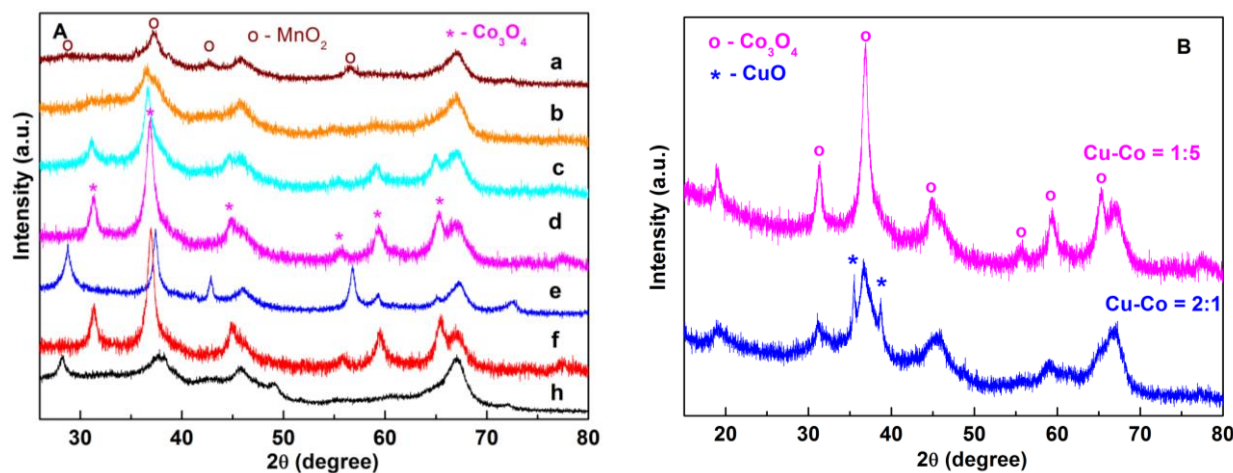


Fig. 1. XRD patterns of the studied samples: (section A)  $\text{Cu-Mn}/\gamma\text{-Al}_2\text{O}_3$  catalysts of Cu/Mn ratio of 1:5 (a); after replacement of Mn by 40 wt.% Co (b); after replacement of Mn by 60 wt.% Co (c); after complete replacement of Mn by Co (d);  $\text{MnO}_2/\gamma\text{-Al}_2\text{O}_3$  (e);  $\text{Co}_3\text{O}_4/\gamma\text{-Al}_2\text{O}_3$  (f), and  $\gamma\text{-Al}_2\text{O}_3$  (h); and (section B):  $\text{Cu-Mn}/\gamma\text{-Al}_2\text{O}_3$  catalysts of Cu/Mn ratio of 1:5 and 2:1 after complete replacement of Mn by Co.

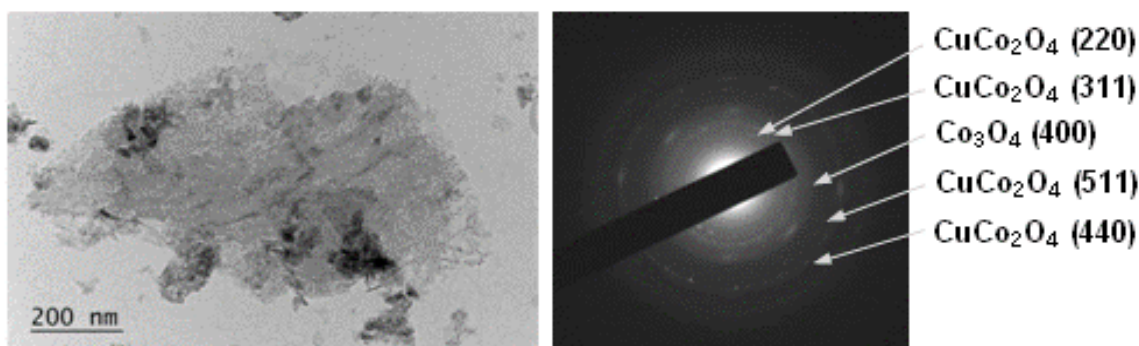


Fig. 2. TEM image and SAED pattern of  $\text{Cu-Mn}/\gamma\text{-Al}_2\text{O}_3$  catalysts of Cu/Mn ratio of 1:5 (60% of Mn replaced by Co) at magnification 25000 x.

$\text{Cu-Mn}/\gamma\text{-Al}_2\text{O}_3$  sample of Cu/Mn ratio of 1:5 modified with 60 wt.% Co are presented in Fig. 2. Phase identification of SAED patterns revealed the presence of a new spinel  $\text{CuCo}_2\text{O}_4$  phase co-existing with  $\text{Co}_3\text{O}_4$  (Table 1).

**Table 1.** Indexing of SAED patterns according to PDF 01-1155 for  $\text{CuCo}_2\text{O}_4$  and PDF 78-1969 for  $\text{Co}_3\text{O}_4$ .

No	D, Å	hkl
1	2.85	(220) $\text{CuCo}_2\text{O}_4$
2	2.43	(311) $\text{CuCo}_2\text{O}_4$
3	2.02	(400) $\text{Co}_3\text{O}_4$
4	1.55	(511) $\text{CuCo}_2\text{O}_4$
5	1.42	(440) $\text{CuCo}_2\text{O}_4$

$\text{Co}_3\text{O}_4$  formation was in agreement with the results of XRD analysis. However, it was suggested that a low amount or rather high dispersion of the  $\text{CuCo}_2\text{O}_4$  spinel phase was the reason for missing signal in the XRD patterns.

### Electron paramagnetic resonance

Figure 3 (A) shows EPR spectra of Cu-Mn/ $\gamma$ -Al<sub>2</sub>O<sub>3</sub> sample of Cu/Mn ratio of 2:1 and 1:5, and of modified samples prepared by replacing manganese by Co in various concentration from 40 to 100%. Due to coupling between electron spin and nuclear spin of the Cu<sup>2+</sup> ions ( $S = 1/2$ ,  $I = 3/2$ ) an EPR spectrum with four parallel and four perpendicular hyperfine components could be expected. Despite this the signal showed a poorly resolved hyperfine splitting for the parallel band characteristic of isolated Cu<sup>2+</sup> ions and unresolved for the perpendicular band. Parameters of the EPR spectra ( $g_{||}$ ,  $g_{\perp}$ , linewidth, and intensity) are listed in Table 2.

It was observed that the  $g$ -values remained constant upon increase of the Co concentrations from 40% to 60% in the Cu-Mn sample of 1:5 ratio. Similar parameters were found in the case of Cu-Mn (2:1) when manganese was completely replaced by cobalt. This result suggests that interactions among Cu and Co ions were rather weak which implied that they were randomly distributed in the Al<sub>2</sub>O<sub>3</sub> matrix without clustering. A weak decrease in the  $g$  values of Cu-Mn (1:5) catalyst with manganese completely replaced by cobalt was related to changes in the chemical environment of the Cu ions in the presence of cobalt and probably due to a new phase formed between copper and cobalt ions.

EPR signal intensity ( $I$ ) and linewidth ( $\Delta H$ ) parameters evolution of the EPR absorption for Cu-Mn (1:5) catalysts are shown in Fig. 3 (B). As seen, increased cobalt content in the samples leads to an increase of  $I$ . The increased signal intensity evidenced a higher total amount of Cu<sup>2+</sup> ions. At the same time,  $\Delta H$  decreased with increasing the cobalt

content of the studied samples and remained relatively constant for higher  $x$  values. This can be related to improved distribution of isolated Cu<sup>2+</sup> ions. Comparing Cu-Co (2:1) and Cu-Co (1:5) intensities and linewidths it was observed that the linewidth of cooper-rich sample was higher than that of manganese-rich sample. This finding could be associated with interacting Cu<sup>2+</sup> ions, which caused a decrease in the amount of isolated Cu<sup>2+</sup> ions in Cu-Co (2:1) in agreement with decreased intensity of the EPR spectra. In many cases, the enhanced catalytic activity is explained by the presence of higher total amount of Cu<sup>2+</sup> ions and increased amount of isolated Cu<sup>2+</sup> ions. However, in this study such a relationship was not observed. It could be suggested that chemical composition, in particular presence of different amounts of Co<sub>3</sub>O<sub>4</sub> and CuCo<sub>2</sub>O<sub>4</sub>, initiated a stronger effect on the catalytic properties.

**Table 2.** Calculated EPR parameters:  $g$ -factor, linewidth and intensity.

Samples	$g_{  }$	$g_{\perp}$	$\Delta H$ , mT	$I$ , a.u.
Cu-Co = 2:1	2.3567	2.0935	29.07	2225.60
Cu-Co = 1:5	2.3560	2.0896	25.39	3251.43
Cu:Mn 1:5 (Co 60%)	2.3567	2.0932	25.39	1862.00
Cu:Mn 1:5 (Co 40%)	2.3565	2.0934	25.47	1792.23

### Temperature-programmed reduction (TPR)

Cu-Mn/ $\gamma$ -Al<sub>2</sub>O<sub>3</sub> samples of Cu/Mn ratio of 2:1 or 1:5, in which manganese was partly or completely replaced by Co<sub>3</sub>O<sub>4</sub>, were studied by temperature-programmed reduction. Fig. 4 (A) shows TPR profiles of CuO-Co<sub>3</sub>O<sub>4</sub>/ $\gamma$ -Al<sub>2</sub>O<sub>3</sub> samples of Cu/Co ratio of 2:1 and 1:5.

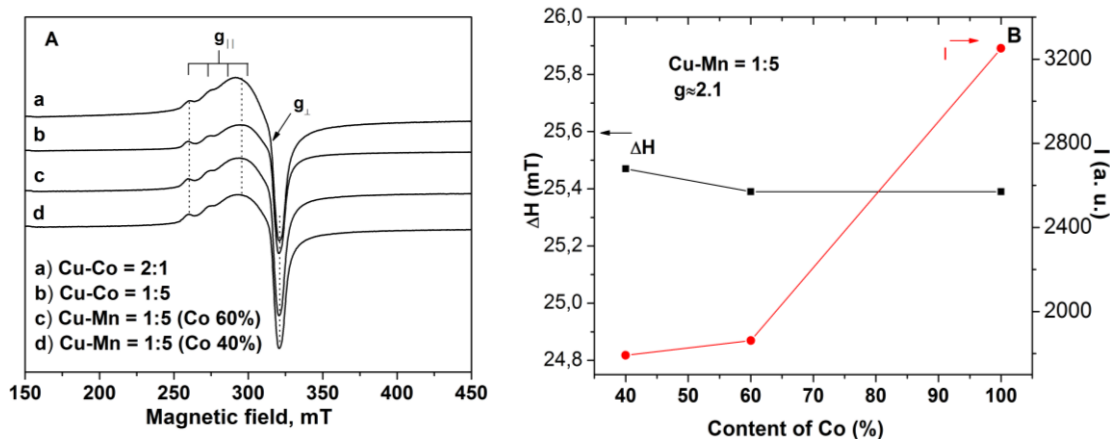


Fig. 3. (A) EPR spectra of Cu-Mn/ $\gamma$ -Al<sub>2</sub>O<sub>3</sub> catalysts of Cu:Mn ratio of 2:1 and 1:5 after partial or total replacement of Mn with Co; (B) dependence of EPR signal intensity and linewidth on cobalt amount in Cu-Mn/ $\gamma$ -Al<sub>2</sub>O<sub>3</sub> of Cu:Mn ratio of 1:5.

The TPR profile of alumina-supported  $\text{Co}_3\text{O}_4$  is also given for comparison. An intense peak with  $T_{\text{max}}$  at about 217 °C registered for the Cu-Co (2:1) sample may be associated with reduction of CuO separate phase whose presence was confirmed by XRD analysis. A small shoulder on the higher-temperature side of the profile could be related to reduction of some of the available  $\text{Co}^{3+}$  ions in  $\text{CuCo}_2\text{O}_4$ . In the cobalt-rich Cu-Co (1:5) sample a complex profile with two maxima at 255 and 284 °C was recorded due to  $\text{Co}_3\text{O}_4 \rightarrow \text{CoO} \rightarrow \text{Co}$  reductive transitions. The better reducibility of this sample was substantially facilitated by the presence of finely divided copper particles.

Fig. 4 (B) shows the TPR profiles of Cu-Mn/ $\gamma\text{-Al}_2\text{O}_3$  samples of Cu/Mn ratio of 1:5 in which Mn was completely replaced (Cu-Co) or partially replaced by 40 and 60 wt.% cobalt. The profile of unmodified Cu-Mn/ $\gamma\text{-Al}_2\text{O}_3$ (1:5) is given for comparison. There is an apparent tendency to shift the temperature maximum to a lower temperature because of partial replacement of Mn by Co (from 290 to 242 °C). Improved reducibility of these samples could contribute to higher catalytic activity.

#### Activity measurements

Fig. 5 displays results obtained in the complete oxidation of CO on Cu-Mn-Co/ $\gamma\text{-Al}_2\text{O}_3$  samples of Cu-Mn ratio of 2:1 (A) and 1:5 (B) where manganese was replaced by cobalt over the entire concentration range from 0 to 100%. The results presented in Fig. 5 (A) indicate that the catalytic reaction started at a temperature of about 80 °C, and full oxidation was reached at 200 °C with all samples except Cu-Co (2:1) (containing 100% of cobalt). For samples containing cobalt within 0–60 wt.%, no clearly notable difference in catalytic activity was observed. The most significant difference in activity was found at 160 °C for samples of 1:5 ratio (Fig. 5, B). At this temperature, the sample modified by 60 wt.% cobalt exhibited over 80% conversion in CO oxidation, while the latter was only 10% over a sample in which manganese was completely replaced by cobalt. The results clearly show that manganese had a favourable effect on catalytic activity and its complete replacement played a negative role on activity. However, the copper-rich sample demonstrated better catalytic properties in the oxidation of CO and methanol. The registered temperatures for 50% conversion of CO ( $T_{50} = 170$  °C) and methanol ( $T_{50} = 175$  °C) were significantly lower than those for Cu-Co (1:5),  $T_{50} = 210$  °C in the oxidation of CO and  $T_{50} = 200$  °C in the oxidation of methanol, respectively. Comparison between the TPR profiles of these two samples revealed improved reducibility of the Cu-Co (2:1) sample and enabled correct explanation of the catalytic results.

Considering methanol oxidation, again no significant difference in activity of the tested samples was observed with both catalysts having a ratio of 2:1 (C) and 1:5 (D). The results demonstrated that full oxidation was achieved at  $T = 220$  °C with all catalysts.

Regarding DME oxidation, there was a tendency of decreasing activity with the increase in cobalt content (Fig.5, E and F). In both groups of catalysts, the highest activity was exhibited by the unmodified samples, and this effect was more pronounced for catalysts of 2:1 ratio. Partial replacement of manganese by 60 wt.% cobalt in catalysts of 1:5 ratio led to a slight increase in activity probably due to formation of spinel structures in the active phase, which was confirmed by TEM measurements.

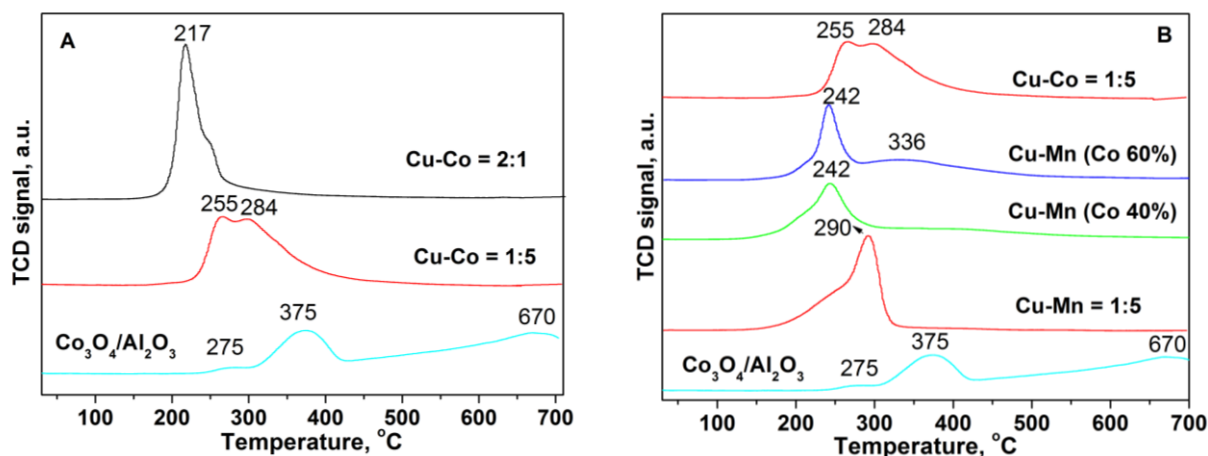


Fig. 4. TPR profiles of Cu-Co/ $\gamma\text{-Al}_2\text{O}_3$  catalysts of Cu:Co ratio of 1:5 and 2:1 (A), and Cu-Mn/ $\gamma\text{-Al}_2\text{O}_3$  catalysts of Cu:Mn ratio of 1:5 after partial or total replacement of Mn by Co (B).

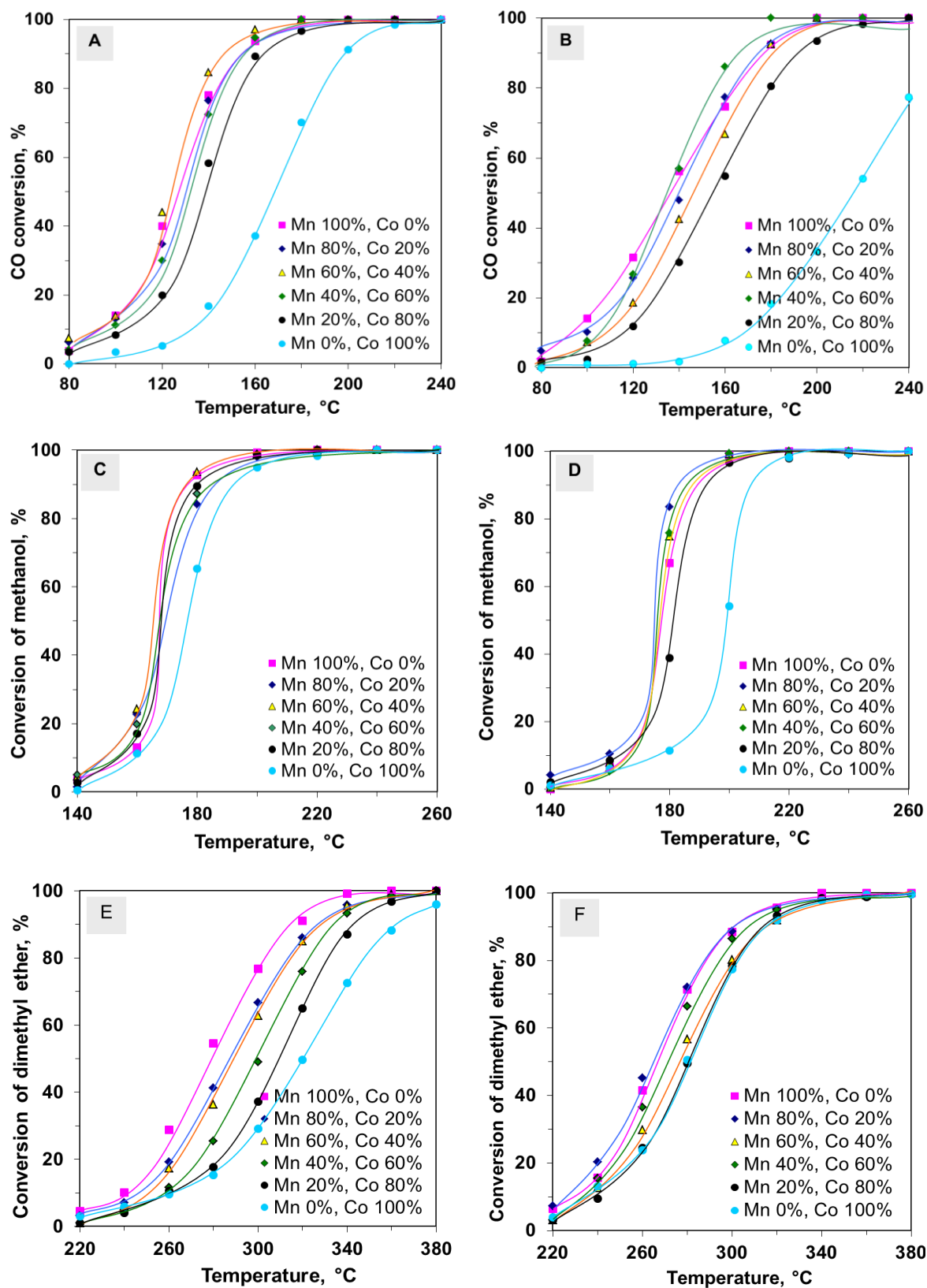


Fig. 5. Temperature dependence: CO oxidation over Cu-Mn-Co/ $\gamma$ -Al<sub>2</sub>O<sub>3</sub> catalyst of Cu:(Mn+Co) ratio of 2:1 (A) and Cu-Mn-Co/ $\gamma$ -Al<sub>2</sub>O<sub>3</sub> catalyst of Cu:(Mn+Co) ratio of 1:5 (B); methanol oxidation over Cu-Mn-Co/ $\gamma$ -Al<sub>2</sub>O<sub>3</sub> catalyst of Cu:(Mn+Co) ratio of 2:1 (C) and Cu-Mn-Co/ $\gamma$ -Al<sub>2</sub>O<sub>3</sub> catalyst of Cu:(Mn+Co) ratio of 1:5 (D); DME oxidation over Cu-Mn-Co/ $\gamma$ -Al<sub>2</sub>O<sub>3</sub> catalyst of Cu:(Mn+Co) ratio of 2:1 (E) and Cu-Mn-Co/ $\gamma$ -Al<sub>2</sub>O<sub>3</sub> catalyst of Cu:(Mn+Co) ratio of 1:5 (F).

Results of the catalytic measurements (Fig. 6, A and B) showed a general trend of increasing activity toward CO and methanol oxidation and decreasing activity toward DME oxidation with the increase of cobalt amount up to 60% for both groups of catalyst. This tendency, however, manifested specific features depending on catalyst composition and nature of the

oxidised gas. The catalytic activity of samples of Cu:(Mn+Co) ratio of 2:1 was gradually changed with increasing cobalt content. The activity of samples of Cu:(Mn+Co) ratio of 1:5 passed through a maximum for 60% manganese replacement by cobalt probably owing to formation of highly dispersed Co-based spinel structures ( $\text{Co}_3\text{O}_4$  and  $\text{CuCo}_2\text{O}_4$ ).

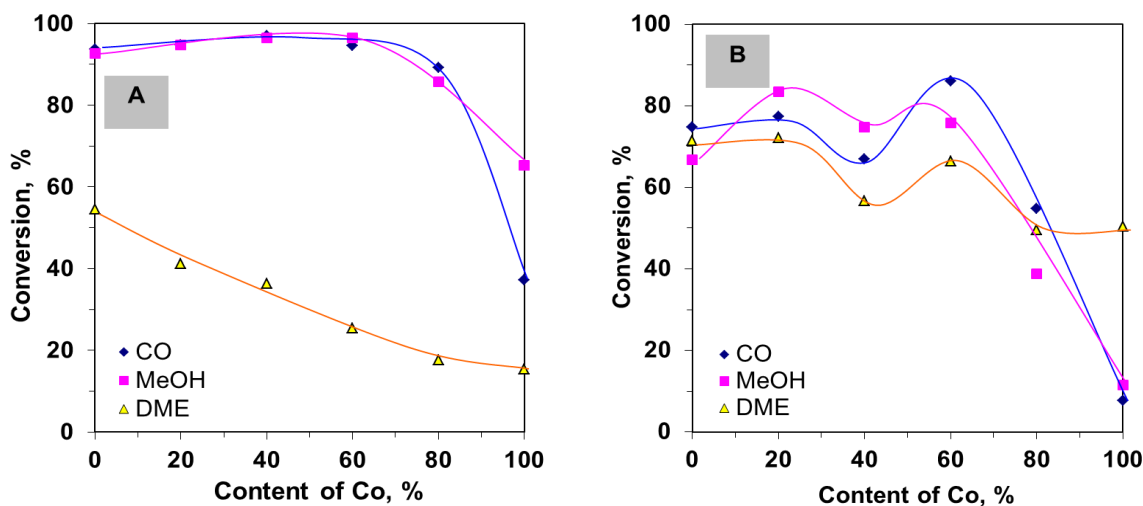


Fig. 6. Effect of manganese replacement by cobalt in Cu-Mn(Co)/ $\gamma$ - $\text{Al}_2\text{O}_3$  catalyst of Cu:(Mn+Co) ratio of 2:1 (A) and Cu:(Mn+Co) ratio of 1:5 (B) on CO,  $\text{CH}_3\text{OH}$ , and DME oxidation ( $T_{\text{CO}} = 160^\circ\text{C}$ ,  $T_{\text{MeOH}} = 180^\circ\text{C}$ ,  $T_{\text{DME}} = 280^\circ\text{C}$ ).

## CONCLUSIONS

The present study demonstrated that chemical composition strongly affected the catalytic properties, this effect being quite variable with regard to different processes. Successful oxidation of CO,  $\text{CH}_3\text{OH}$ , and DME was achieved over a sample of Cu-Mn ratio of 1:5 and partial replacement of manganese by 60 wt.% cobalt in the active component. Analysis of XRD and TEM data (including SAED) indicated at least three compounds in this sample:  $\text{Co}_3\text{O}_4$ ,  $\text{MnO}_2$ , and  $\text{CoCu}_2\text{O}_3$ . Study of the effect of modification by cobalt upon variation of its content in Cu-Mn/ $\gamma$ - $\text{Al}_2\text{O}_3$  showed that a Cu-Mn-Co)/ $\gamma$ - $\text{Al}_2\text{O}_3$  composition of Cu:(Mn+Co) 1:5 ratio with 60 wt.% Co appeared beneficial for catalytic performance. The activity of the best-performing sample could also be related to improved reducibility.

**Acknowledgment:** The authors affiliated at Agricultural University in Plovdiv acknowledge the financial support by Agricultural University Science Fund (Project 6/16).

## REFERENCES

- S. Hosseini, D. Salari, A. Niaei, F. Deganello, G. Pantaleo, Pejmanhojati, *J. Envir. Sci. Health, Part A*, **46**, 291(2011).
- A. Ulukardesler, *Energy Sources, Part A*, **35**, 1218 (2013).
- G. Rattan, R. Prasad, R. C. Katyal, 21<sup>th</sup> Int. Conf. Thai Inst. Chem. Engn. Appl. Chem. (TICHe 2011), Hatyai, Songkhla, Thailand, 2011.
- W. Tang, W. Li, D. Li, G. Liu, X. Wu, Y. Chen, *Catal. Lett.*, **144**, 1900 (2014).
- T. Tsoncheva, K. Ivanov, D. Dimitrov, *Can. J. Chem.*, **5**, 583 (2011).
- B. White, PhD Thesis, Graduate School of Arts and Sciences, Columbia University, New York (2007).
- R. Prasad, P. Singh, *Catal. Rev.: Sci. Eng.*, **54**, 224 (2012).
- B. Faure, P. Alphonse, *Appl. Catal. B*, **180**, 715 (2016).
- S. Todorova, I. Yordanova, A. Naydenov, H. Kolev, Z. Cherkezova-Zhelev, K. Tenchev, B. Kunev, *Rev. Roum. Chim.*, **59**, 259 (2014).
- E. C. Njagi, C. H. Chen, H. Genuino, H. Galindo, H. Huang, S. L. Suib, *Appl. Catal. B*, **99**, 103 (2010).
- L. N. Cai, Y. Guo, A.-H. Lu, P. Branton, W.-C. Li, *J. Molec. Catal. A*, **360**, 35 (2012).
- G. Hutchings, A. Mirzaei, R. Joyner, M. Siddiqui, S. Taylor, *Appl. Catal. A*, **166**, 143 (1998).
- S. Behar, P. Gonzalez, P. Aguilhon, F. Quignard, D. Szwierczynski, *Catal. Today*, **189**, 35 (2012).
- M. Morales, B. Barbero, L. Cadus, *Appl. Catal. B*, **67**, 229 (2006).
- K. Ivanov, E. Kolentsova, D. Dimitrov, *Int. J. Chem.*

- Molec. Nuclear Mater. Metallurg. Eng.*, **9**, 548 (2015).  
14. K.-D. Zhi, Q.-S. Liu, Y.-G. Zhang, S. He, R.-X. He, *J. Fuel Chem. Technol.*, **38** (4), 445 (2010).  
15. J. Papavasiliou, G. Avgouropoulos, T. Ioannides, *Catal. Commun.*, **6**, 497 (2005).

## КАТАЛИТИЧНО ОЧИСТВАНЕ НА ОТПАДЪЧНИ ГАЗОВЕ ОТ СО И ЛЕТЛИВИ ОРГАНИЧНИ СЪЕДИНЕНИЯ ВЪРХУ Cu-Mn/ $\gamma$ -Al<sub>2</sub>O<sub>3</sub> КАТАЛИЗАТОРИ МОДИФИЦИРАНИ С КОБАЛТ

Е. Н. Коленцова<sup>1</sup>, Д. Я. Димитров<sup>1</sup>, Д. Б. Карашанова<sup>2</sup>, Й. Г. Каракирова<sup>3</sup>, П. Цв. Петрова<sup>3</sup>,  
Т. Т. Табакова<sup>3\*</sup>, Г. В. Авдеев<sup>4</sup>, К. И. Иванов<sup>1</sup>

<sup>1</sup> Катедра „Обща химия“, Аграрен университет, 4000 Пловдив, България

<sup>2</sup> Институт по катализ, Българска академия на науките, 1113 София, България

<sup>3</sup> Институт по оптични материали и технологии, Българска академия на науките, 1113 София, България

<sup>4</sup> Институт по физикохимия, Българска академия на науките, 1113 София, България

Постъпила на 1 февруари 2018 г.; Преработена на 11 март 2018 г.

(Резюме)

Производството на формалдехид чрез селективно окисление на метанол е важен промишлен процес. Основните странични продукти в отпадните газове са СО и диметилов етер (ДМЕ). Понастоящем дизайнът на нови каталитични материали с подобрена ефективност за отстраняване на замърсители на въздуха е предмет на значителни проучвания. Целта на това изследване е да се съчетаят предимствата на Cu-Mn и Cu-Co каталитични системи, като се получи нов смесен Cu-Mn-Co катализатор с висока активност и селективност за едновременно окисление на СО, метанол и ДМЕ. Катализаторните образци са охарактеризирани с рентгено-структурен анализ, трансмисионна електронна микроскопия, електронен парамагнитен резонанс и температурно-програмирана редукция.